Mathematical Morphology and Artificial Intelligence

Isabelle Bloch, Samy Blusseau, Ramón Pino Pérez

Tutorial at ECAI 2020

Outline

How can mathematical morphology be associated with AI, in symbolic, semi-qualitative and machine learning frameworks?

1. Introduction to mathematical morphology
2. Mathematical morphology and logics
3. Mathematical morphology and spatial reasoning
4. Mathematical morphology and deep learning

Note: only a small part of mathematical morphology will be described, and a small part of AI as well...

1. Introduction to mathematical morphology

Lattices and information processing

Lattices: core mathematical structure in many information processing problems.

Examples:

- soft computing (fuzzy sets, bipolar information),
- knowledge representation,
- logics,
- formal concept analysis,
- automated reasoning,
- decision making,
- image processing and understanding,
- information retrieval,
- etc.

Mathematical morphology on complete lattices.

Mathematical morphology for spatial information

Matheron [Matheron, 1967, Matheron, 1975], Serra [Serra, 1982, Serra, 1988]

- A theory of space.
- Widely used in image processing and interpretation.
- At different levels (local, regional, structural...).
- For different tasks (filtering, enhancement, segmentation, interpretation, spatial knowledge modeling...).

Filtering

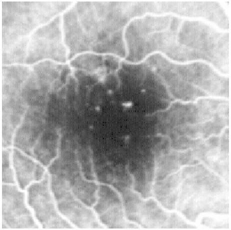

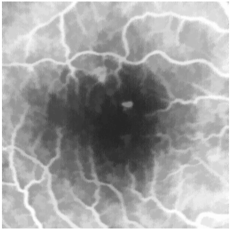

Segmentation

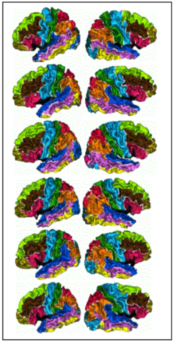

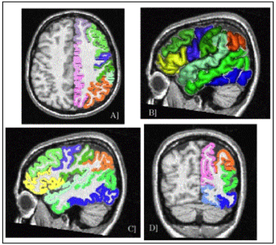

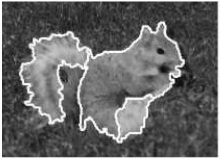

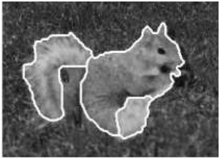

Interpretation

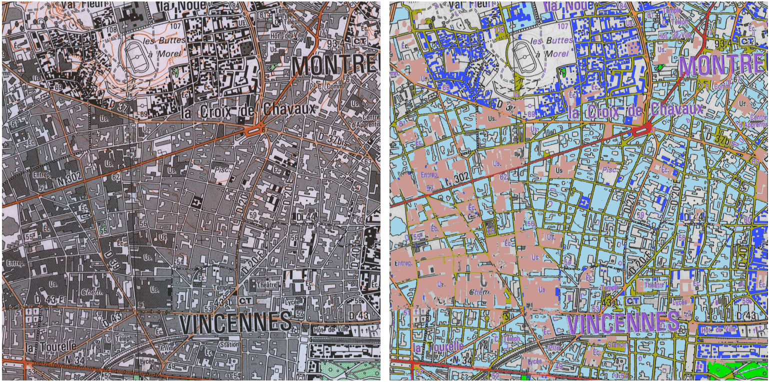

Knowledge modeling What is the region *to the right of R*? Is *B to the right of R (and to which degree)*?

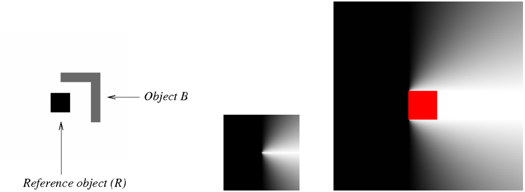

Spatial reasoning

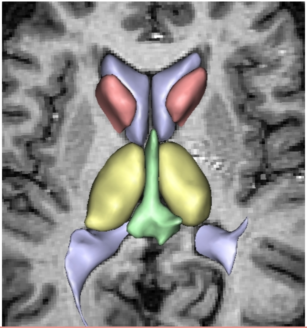

Algebraic dilations and erosions - [Heijmans and Ronse, 1990]

Complete lattices $(\mathcal{T}, \leq)$, $(\mathcal{T}', \leq')$
Example: $(\mathcal{P}(E), \subseteq)$ *for a set* E

Algebraic dilation: $\delta : \mathcal{T} \to \mathcal{T}'$ such that

$$\forall (x_i) \in \mathcal{T},\ \delta(\vee_i x_i) = \vee'_i \delta(x_i)$$

Algebraic erosion: $\varepsilon : \mathcal{T}' \to \mathcal{T}$ such that

$$\forall (x_i) \in \mathcal{T}',\ \varepsilon(\wedge'_i x_i) = \wedge_i \varepsilon(x_i)$$

Properties:

- $\delta(0) = 0'$ (in $\mathcal{P}(E), 0 = \emptyset$)
- $\varepsilon(I') = I$ (in $\mathcal{P}(E), I = E$)
- δ increasing, ε increasing
- in $\mathcal{P}(\mathbb{R}^n)$, $\delta(X) = \cup_{x \in X} \delta(\{x\})$

Adjunctions

$\delta : \mathcal{T} \rightarrow \mathcal{T}'$, $\varepsilon : \mathcal{T}' \rightarrow \mathcal{T}$, (ε, δ) adjunction if:

$$\forall x \in \mathcal{T}, \forall y \in \mathcal{T}',\ \delta(x) \leq' y \Leftrightarrow x \leq \varepsilon(y)$$

Properties:

- $\delta(0) = 0'$ and $\varepsilon(I') = I$
- (ε, δ) adjunction $\Rightarrow \varepsilon =$ algebraic erosion and $\delta =$ algebraic dilation
- δ increasing $=$ algebraic dilation iff $\exists \varepsilon$ such that (ε, δ) is an adjunction $\Rightarrow \varepsilon =$ algebraic erosion and $\varepsilon(x) = \bigvee\{y \in \mathcal{T},\ \delta(y) \leq' x\}$
- ε increasing $=$ algebraic erosion iff $\exists \delta$ such that (ε, δ) is an adjunction $\Rightarrow \delta =$ algebraic dilation and $\delta(x) = \bigwedge\{y \in \mathcal{T}',\ \varepsilon(y) \geq x\}$
- $\varepsilon\delta \geq Id$ and $\delta\varepsilon \leq Id'$
- $\varepsilon\delta\varepsilon = \varepsilon$ and $\delta\varepsilon\delta = \delta$
- $\varepsilon\delta\varepsilon\delta = \varepsilon\delta$ and $\delta\varepsilon\delta\varepsilon = \delta\varepsilon$
- δ and ε increasing such that $\delta\varepsilon \leq Id'$ and $\varepsilon\delta \geq Id \Rightarrow (\varepsilon, \delta)$ adjunction

Morphological dilations and erosions

- On the lattice of the subsets of $\mathbb{R}^n$ or $\mathbb{Z}^n$, with inclusion:

$$\delta(X) = \cup_{x \in X} \delta(\{x\})$$

- + invariance under translation
  $\Rightarrow \exists B,\ \delta(X) = D(X, B) = \{x, \check{B}_x \cap X \neq \emptyset\}$ (with $B_x = x + B$).
- B = structuring element (neighborhood, binary relation).
- Same result on the lattice of functions.
- Similar results for erosion: $\exists B,\ \varepsilon(X) = E(X, B) = \{x, B_x \subseteq X\}$.

Derived operators: opening, closing, conditional (geodesic) operations, gradient...

Relaxing the assumption on invariance under translation: structuring elements varying in space (ex: projective geometry, omnidirectional images...).

A simple example

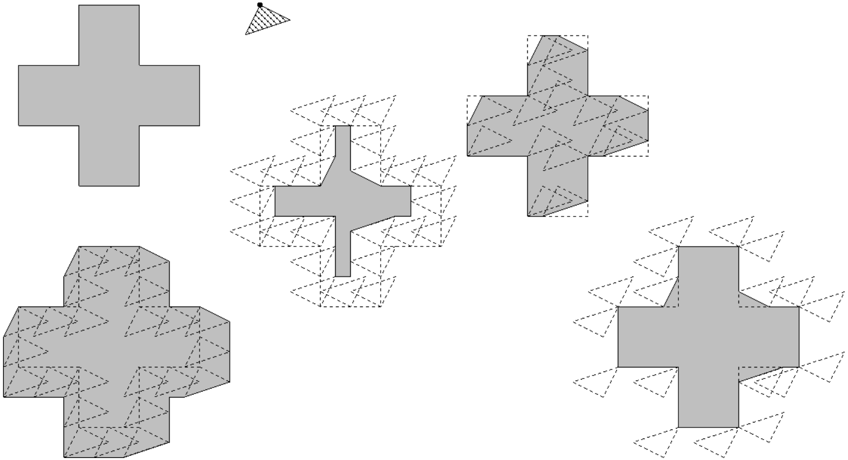

(Illustration: C. Ronse [Bloch et al., 2007])

2. Mathematical morphology and logics

Morpho-Logics: first steps

Mathematical morphology on logical formulas, via the models, in propositional logic [Bloch and Lang, 2000, Bloch and Lang, 2002].

- Set of all models of a formula φ: $[\![\varphi]\!] = \{\omega \in \Omega \mid \omega \models \varphi\}$
- Lattice structure on the set of all models $\Leftrightarrow$ lattice structure on the set of formulas (up to an equivalence relation).
- $[\![\varphi \vee \psi]\!] = [\![\varphi]\!] \cup [\![\psi]\!]$,
- $[\![\varphi \wedge \psi]\!] = [\![\varphi]\!] \cap [\![\psi]\!]$,
- $[\![\varphi]\!] \subseteq [\![\psi]\!]$ iff $\varphi \models \psi$, and φ is consistent iff $[\![\varphi]\!] \neq \emptyset$
- Algebraic dilations and erosions as in any complete lattice.

Morphological dilation of a formula φ with a structuring element B:

$$[\![\delta_B(\varphi)]\!] = \delta_B([\![\varphi]\!]) = \{\omega \in \Omega \mid \check{B}_\omega \wedge \varphi \textit{ consistent}\}.$$

Morphological erosion:

$$[\![\varepsilon_B(\varphi)]\!] = \varepsilon_B([\![\varphi]\!]) = \{\omega \in \Omega \mid B_\omega \models \varphi\}.$$

B: a relation between worlds, e.g. neighborhood, distance.

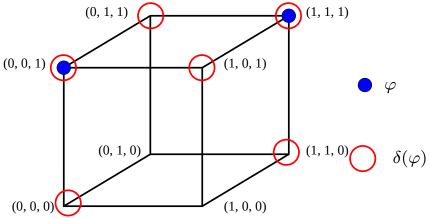

Example of a dilation of size 1 (Hamming distance):
$\varphi = (a \wedge b \wedge c) \vee (\neg a \wedge \neg b \wedge c)$ and $\delta(\varphi) = (\neg a \vee b \vee c) \wedge (a \vee \neg b \vee c)$.

Use for typical reasoning problems in AI
[Bloch et al., 2001, Bloch et al., 2004, Bloch et al., 2006, Bloch et al., 2018].

- Revision.
- Merging (fusion).
- Abductive reasoning.
- Mediation.

Using dilations and erosions
Morphological partial ordering: stratification of the models from successive dilations and erosions.

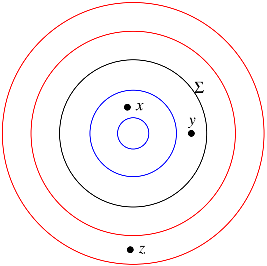

Example: $x \preceq_f y \preceq_f z$

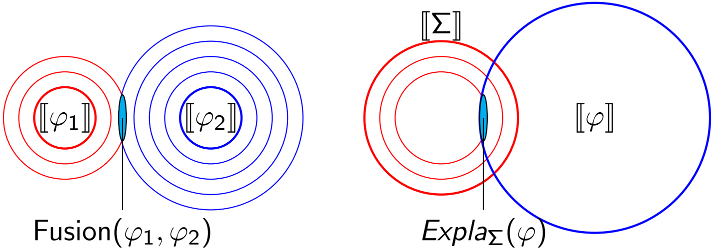
⟦φ_1⟧
⟦φ_2⟧
Fusion(φ_1, φ_2)
⟦Σ⟧
⟦φ⟧
$Expla_\Sigma(\varphi)$

Belief revision

Revision of φ by ψ (new piece of information): $\varphi \circ \psi$ (with minimal change on the initial set of beliefs)

$$\varphi \circ \psi = \delta^n(\varphi) \wedge \psi$$

with $n = \min\{k \in \mathbb{N} \mid \delta^k(\varphi) \wedge \psi \text{ is consistent}\}$.

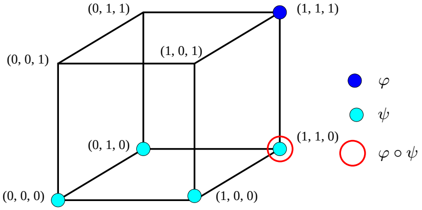

Satisfies the AGM postulates [Alchourron et al., 1985] in Katsuno and Mendelzon's model [Katsuno and Mendelzon, 1991].

Belief merging

Morphological expressions of several operators for logical fusion of beliefs $\{\varphi_1 ... \varphi_m\}$ under integrity constraint μ, satisfying the rationality postulates of [Konieczny and Pino Pérez, 2011]:

$$\Delta_\mu^{max}(\varphi_1, ..., \varphi_m) = \delta^n(\varphi_1) \wedge \delta^n(\varphi_2) \wedge ... \wedge \delta^n(\varphi_m) \wedge \mu$$

where $n = \min\{k \in \mathbb{N} \mid \delta^k(\varphi_1) \wedge ... \wedge \delta^k(\varphi_m) \wedge \mu$ is consistent$\}$.

$$\Delta_\mu^{\Sigma}(\varphi_1, ..., \varphi_m) = \bigvee_{(n_1, ..., n_m)} \delta^{n_1}(\varphi_1) \wedge \delta^{n_2}(\varphi_2) \wedge ... \wedge \delta^{n_m}(\varphi_m) \wedge \mu$$

where $\sum_{i=1}^m n_i$ is minimal with $\delta^{n_1}(\varphi_1) \wedge \delta^{n_2}(\varphi_2) \wedge ... \wedge \delta^{n_m}(\varphi_m) \wedge \mu$ consistent.

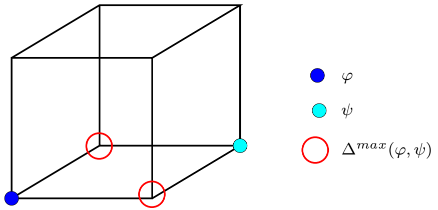

Agent 1:

- prefers to travel in Spain: $\varphi_1 = Spain$.

Agent 2:

- prefers to travel in Morocco: $\varphi_2 = Morocco$.

$\Rightarrow$ conflict!

Extending preferences using dilations:

$$\delta(\varphi_1) = \mathit{Spain} \vee \mathit{France} \vee \mathit{Portugal} \vee \mathit{Morocco}$$

$$\delta(\varphi_2) = \mathit{Morocco} \vee \mathit{Algeria} \vee \mathit{Portugal} \vee \mathit{Spain}$$

Fusion:

$$\Delta(\varphi_1, \varphi_2) = \delta(\varphi_1) \wedge \delta(\varphi_2) = \mathit{Spain} \vee \mathit{Portugal} \vee \mathit{Morocco}.$$

$\Rightarrow$ Solution for travelling in the set of models of this formula.

Mediation

Symmetric merging is not always fair:

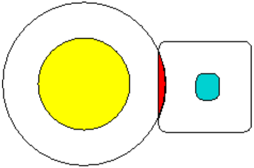

⇒ New mediation operators based on morphological median.

Abduction

- Explanation γ of α: $\Sigma \cup \{\gamma\} \vdash \alpha$.
- Abduction: finding the best explanations.
- Rationality postulates of [Pino Pérez and Uzcátegui, 2003].
- General idea: finding the most central models in Σ or in $\Sigma \wedge \alpha$.

$\Rightarrow$ Using morphological erosions:

$$\alpha \rhd_1^{\ell ne} \gamma \quad \overset{def}{\Leftrightarrow} \quad \gamma \equiv_\Sigma \varepsilon_\ell(\Sigma \wedge \alpha)$$

$$\alpha \rhd_2^{\ell ne} \gamma \quad \overset{def}{\Leftrightarrow} \quad \gamma \vdash_\Sigma \varepsilon_\ell(\Sigma \wedge \alpha)$$

$$\alpha \rhd^{\ell c} \gamma \quad \overset{def}{\Leftrightarrow} \quad \gamma \vdash_\Sigma \varepsilon_{\ell c}(\Sigma, \alpha) \wedge \alpha$$

Choice of the structuring element $\Rightarrow$

- explanation as a disjunction (OR),
- explanation as a conjunction (AND),
- explanation as an exclusive disjunction (XOR).

Other logics

First order logic, with application to merging
[Gorogiannis and Hunter, 2008b, Gorogiannis and Hunter, 2008a]
Modal logics [Bloch, 2002]:

Accessibility relation / Structuring element – $\Box$ / ε – $\Diamond$ / δ

Description logics [Hudelot et al., 2008, Atif et al., 2014]: δ and ε as binary predicates, ontological reasoning.

Satisfaction systems and institutions
[Aiguier et al., 2018a, Aiguier et al., 2018b, Aiguier and Bloch, 2019]:

- General framework for many logics.
- Revision based on relaxations.
- Abduction based on cuttings and retractions.
- Dual operators from dilations and erosions.
- Towards spatial reasoning.

3. Mathematical morphology and spatial reasoning
Qualitative (symbolic) and semi-qualitative frameworks

Spatial reasoning: Knowledge representation and reasoning on spatial entities and spatial relationships

Spatial reasoning using modal morpho-logic

Examples in mereotopology (with $\Box \equiv \varepsilon$ and $\Diamond \equiv \delta$):

- tangential part: $\varphi \rightarrow \psi$ and $\Diamond\varphi \wedge \neg\psi$ consistent, or $\varphi \rightarrow \psi$ and $\varphi \wedge \neg\Box\psi$ consistent

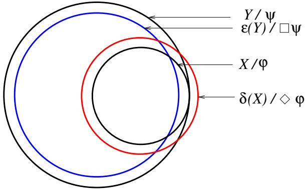

- non tangential part: $\Diamond\varphi \rightarrow \psi$, or $\varphi \rightarrow \Box\psi$
- external connection (adjacency): $\varphi \wedge \psi$ inconsistent and $\Diamond\varphi \wedge \psi$ consistent (or $\varphi \wedge \Diamond\psi$ consistent)

Further links between mathematical morphology and RCC: [Bloch et al., 2007, Bloch, 2017, Landini et al., 2019]

Abductive reasoning: example in image understanding

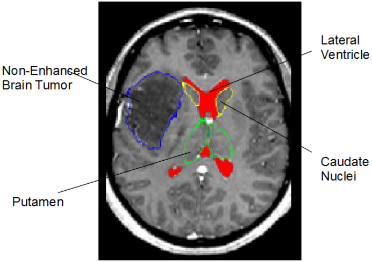

Pathological brain with a tumor

$$\mathcal{K} \models (\gamma \rightarrow \mathcal{O})$$

Compute the "best" explanation to the observations taking into account the expert knowledge (e.g. formalized in description logic) [Atif et al., 2014]

Tbox:

$$
\begin{array}{rcl}
Brain & \sqsubseteq & HumanOrgan \\
CerebralHemisphere & \sqsubseteq & BrainAnatomicalStructure \\
PeripheralCerebralHemisphere & \sqsubseteq & CerebralHemisphereArea \\
SubCorticalCerebralHemisphere & \sqsubseteq & CerebralHemisphereArea \\
GreyNuclei & \sqsubseteq & BrainAnatomicalStructure \\
LateralVentricle & \sqsubseteq & BrainAnatomicalStructure \\
BrainTumor & \sqsubseteq & Disease \sqcap \exists hasLocation.Brain \\
SmallDeformingTumor & \equiv & BrainTumor \sqcap \exists hasBehavior.Infiltrating \\
 & & \sqcap \exists hasEnhancement.NonEnhanced \\
SubCorticalSmallDeformingTumor & \equiv & SmallDeformingTumor \sqcap \\
 & & \exists hasLocation.SubCorticalCerebralHemisphere \\
 & & \sqcap \exists closeTo.GreyNuclei \\
PeripheralSmallDeformingTumor & \equiv & BrainTumor \sqcap \\
 & & \exists hasLocation.PeripheralCerebralHemisphere \\
 & & \sqcap \exists farFrom.LateralVentricle \\
LargeDeformingTumor & \equiv & BrainTumor \sqcap \\
 & & \exists hasLocation.CerebralHemisphere \\
 & & \sqcap \exists hasComponent.Edema \\
 & & \sqcap \exists hasComponent.Necrosis \\
 & & \sqcap \exists hasEnhancement.Enhanced
\end{array}
$$

$$
\begin{aligned}
\mathit{DiseasedBrain} &\equiv \mathit{Brain} \sqcap \exists \mathit{isAlteredBy}.\mathit{Disease} \\
\mathit{TumoralBrain} &\equiv \mathit{Brain} \sqcap \exists \mathit{isAlteredBy}.\mathit{BrainTumor} \\
\mathit{SmallDeformingTumoralBrain} &\equiv \mathit{Brain} \sqcap \exists \mathit{isAlteredBy}.\mathit{SmallDeformingTumor} \\
\mathit{LargeDeformingTumoralBrain} &\equiv \mathit{Brain} \sqcap \exists \mathit{isAlteredBy}.\mathit{LargeDeformingTumor} \\
\mathit{PeripheralSmallDeformingTumoralBrain} &\equiv \mathit{Brain} \sqcap \exists \mathit{isAlteredBy}.\mathit{PeripheralSmallDeformingTumor} \\
\mathit{SubCorticalSmallDeformingTumoralBrain} &\equiv \mathit{Brain} \sqcap \exists \mathit{isAlteredBy}.\mathit{SubCorticalSmallDeformingTumor} \\
&\ldots
\end{aligned}
$$

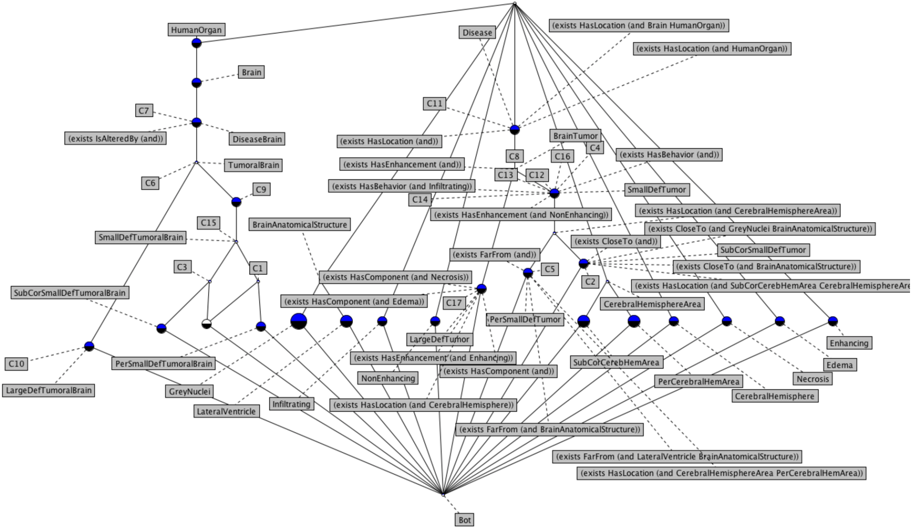
HumanOrgan
Brain
C7
(exists IsAlteredBy (and))
DiseaseBrain
TumoralBrain
C6
C9
C15
SmallDefTumoralBrain
C3
C1
SubCorSmallDefTumoralBrain
C10
LargeDefTumoralBrain
PerSmallDefTumoralBrain
GreyNuclei
LateralVentricle
Infiltrating
BrainAnatomicalStructure
Disease
(exists HasLocation (and Brain HumanOrgan))
(exists HasLocation (and HumanOrgan))
C11
(exists HasLocation (and))
BrainTumor
C4
C8
C16
(exists HasBehavior (and))
(exists HasEnhancement (and))
C13
C12
(exists HasBehavior (and Infiltrating))
SmallDefTumor
C14
(exists HasEnhancement (and NonEnhancing))
(exists HasLocation (and CerebralHemisphereArea))
(exists CloseTo (and GreyNuclei BrainAnatomicalStructure))
(exists CloseTo (and))
SubCorSmallDefTumor
(exists FarFrom (and))
(exists CloseTo (and BrainAnatomicalStructure))
C5
(exists HasComponent (and Necrosis))
C2
(exists HasLocation (and SubCorCerebHemArea CerebralHemisphereAre
(exists HasComponent (and Edema))
C17
CerebralHemisphereArea
PerSmallDefTumor
LargeDefTumor
Enhancing
(exists HasEnhancement (and Enhancing))
SubCorCerebHemArea
Edema
(exists HasComponent (and))
NonEnhancing
Necrosis
PerCerebralHemArea
CerebralHemisphere
(exists HasLocation (and CerebralHemisphere))
(exists FarFrom (and BrainAnatomicalStructure))
(exists FarFrom (and LateralVentricle BrainAnatomicalStructure))
(exists HasLocation (and CerebralHemisphereArea PerCerebralHemArea))
Bot

Abox:

$$
\begin{aligned}
t_1 &: \textit{BrainTumor} \\
e_1 &: \textit{NonEnhanced} \\
l_1 &: \textit{LateralVentricle} \\
p_1 &: \textit{PeripheralCerebralHemisphere} \\
(t_1, e_1) &: \textit{hasEnhancement} \\
(t_1, l_1) &: \textit{farFrom} \\
(t_1, p_1) &: \textit{hasLocation}
\end{aligned}
$$

Most specific concept:

$$
\begin{aligned}
C \equiv \textit{BrainTumor} \sqcap \exists \textit{hasEnhancement}.\textit{NonEnhanced} \sqcap \\
\exists \textit{farFrom}.\textit{LateralVentricle} \sqcap \\
\exists \textit{hasLocation}.\textit{PeripheralCerebralHemisphere}
\end{aligned}
$$

Concept abduction problem $\langle \mathcal{K}, C \rangle$: $\gamma \sqsubseteq_{\mathcal{K}} C$

Possible explanation set:
$\{$*DiseasedBrain*, $\exists$*isAlteredBy*.$\top$, *SmallDeformingTumoralBrain*,
PeripheralSmallDeformingTumoralBrain...$\}$.

A preferred solution with respect to some minimality criteria:

$$\boxed{\gamma \equiv PeripheralSmallDeformingTumoralBrain}$$

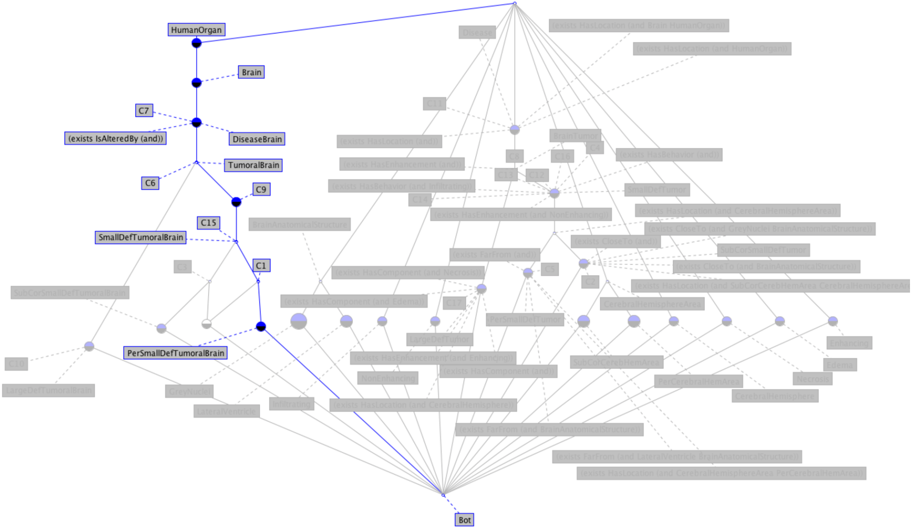
HumanOrgan
Brain
C7
(exists IsAlteredBy (and))
DiseaseBrain
TumoralBrain
C6
C9
C15
SmallDefTumoralBrain
C1
PerSmallDefTumoralBrain
Bot

Semi-qualitative framework: fuzzy sets

- Modeling spatial imprecision (objects, spatial relations).
- Fusion.
- Reasoning.

Fuzzy sets in a nutshell (Zadeh, 1965)

- Space $\mathcal{S}$ (image space, space of characteristics, etc.).
- Fuzzy set: $\mu : \mathcal{S} \rightarrow [0, 1]$ – $\mu(x) =$ membership degree of x to μ.
- Set theoretical operations: complementations, conjunctions (t-norms), disjunctions (t-conorms).
- Logics, aggregation and fusion operators...

Example: spatial fuzzy set

- $\mathcal{S}$: $\mathbb{R}^3$ or $\mathbb{Z}^3$ in the digital case
- $\mu : \mathcal{S} \rightarrow [0, 1]$ - $\mu(x) =$ degree to which x belongs to the fuzzy object

Fuzzy spatial relations [Bloch, 2005]

- Set theoretical relations.
- Topology: connectivity, connected components, neighborhood, boundaries, adjacency.
- Distances.
- Relative direction.
- More complex relations: between, along, parallel, around...

Modeling fuzzy spatial relations: example

Mathematical models: combining fuzzy sets and mathematical morphology.

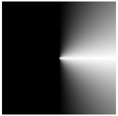

ν_{right}

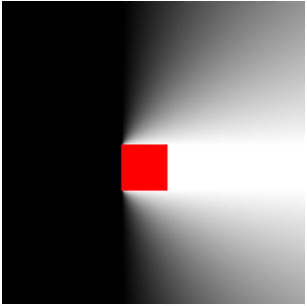

$\delta_{\nu_{right}}(square)$

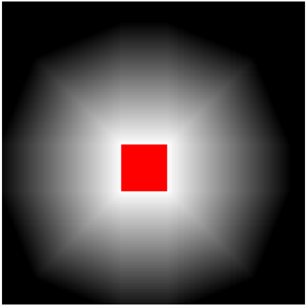

$\delta_{\nu_{close}}(square)$

Types of representations

- number in $\mathbb{R}^+$ (or in $[0, 1]$)
- interval
- fuzzy number, fuzzy interval, distribution
- spatial fuzzy sets
- linguistic value
- logical formula

$\Rightarrow$ unifying framework of fuzzy set theory

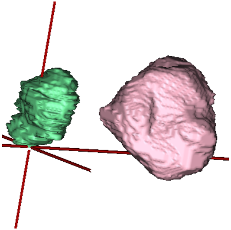

$d_{min} = 17, d_{Haus} = 80$

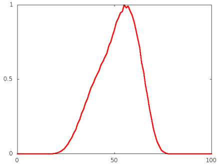

Reasoning

- Ontological representations:
  - concepts, relations, roles...
  - semantic gap between abstract concepts and image features
  - linguistic variable
- Reasoning for image understanding:
  - graphs and hypergraphs, conceptual graphs
  - matching
  - constraint satisfaction problems
  - logics

Example in brain imaging

- Concepts:
  - brain: part of the central nervous system located in the head
  - caudate nucleus: a deep gray nucleus of the telencephalon involved with control of voluntary movement
  - glioma: tumor of the central nervous system that arises from glial cells
  - ...
- Spatial organization:
  - the left caudate nucleus is inside the left hemisphere
  - it is close to the lateral ventricle
  - it is outside (left of) the left lateral ventricle
  - it is above the thalamus, etc.
  - ...
- Pathologies: relations are quite stable, but more flexibility should be allowed in their semantics

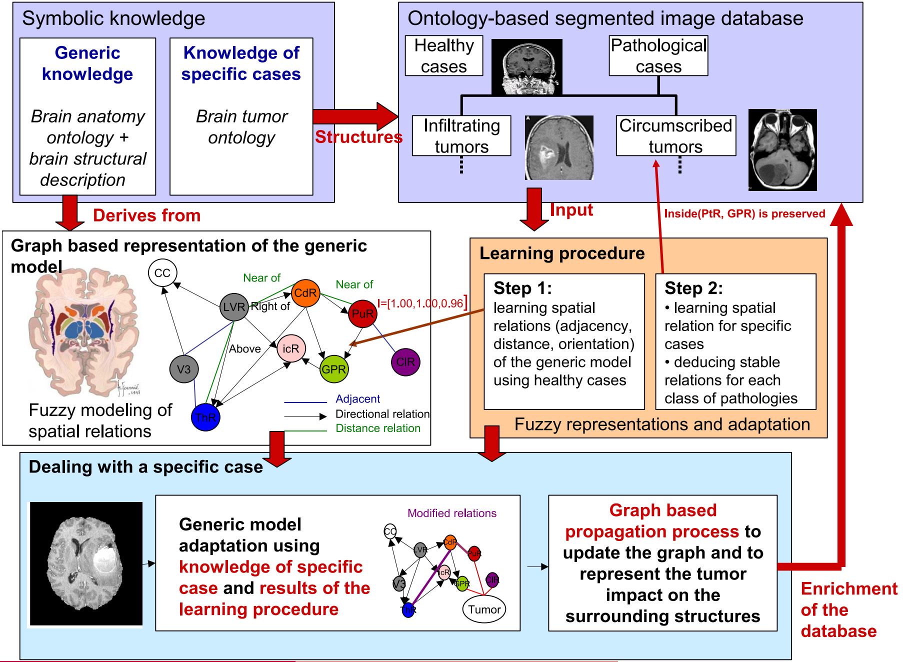
Symbolic knowledge
Generic knowledge
Brain anatomy ontology + brain structural description
Knowledge of specific cases
Brain tumor ontology
Structures
Ontology-based segmented image database
Healthy cases
Pathological cases
Infiltrating tumors
Circumscribed tumors
Derives from
Input
Inside(PtR, GPR) is preserved
Graph based representation of the generic model
Fuzzy modeling of spatial relations
CC
Near of
CdR
Near of
LVR
Right of
PuR
I=[1.00,1.00,0.96]
Above
icR
GPR
CIR
V3
ThR
Adjacent
Directional relation
Distance relation
Learning procedure
Step 1:
learning spatial relations (adjacency, distance, orientation) of the generic model using healthy cases
Step 2:
• learning spatial relation for specific cases
• deducing stable relations for each class of pathologies
Fuzzy representations and adaptation
Dealing with a specific case
Generic model adaptation using knowledge of specific case and results of the learning procedure
Modified relations
Tumor
Graph based propagation process to update the graph and to represent the tumor impact on the surrounding structures
Enrichment of the database

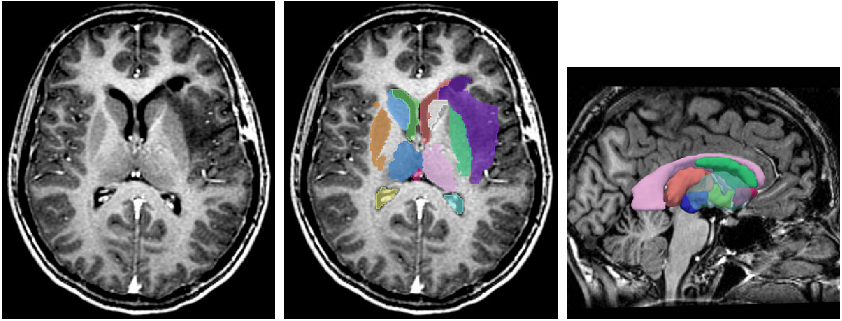

[Fouquier et al., 2012, Nempont et al., 2013]

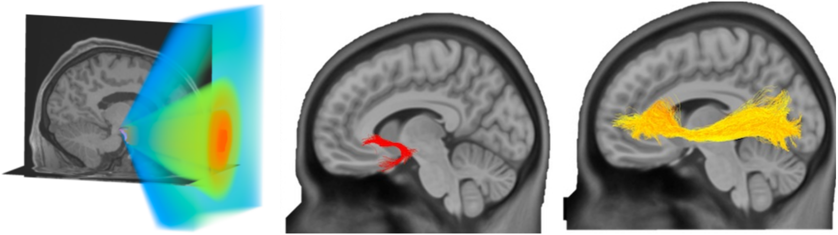

[Delmonte et al., 2018]

- Descriptions:
  - Sacral Plexus = (crossing(VertebralCanalL5) and not anterior of(ObturatorMuscle)) or (crossing(SacralHoleS1) and not (anterior of(LevatorAniMuscle) ...
  - S4 = crossing SacralHoleS4 and crossing SacrumCanal
  - L5 = anterior of Sacrum and ...
  - ...
- Spatial relations: fuzzy models and mathematical morphology.
- Fuzzy connectives.
- Aggregation and final decision.

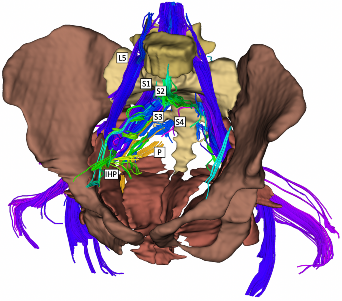

[Muller et al., 2019]

Conceptual graphs and complex spatial relations [Vanegas et al., 2016]

(a) Example image.

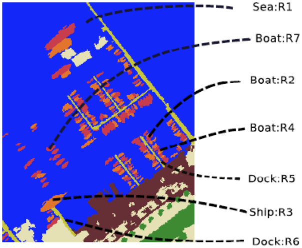

(b) Labeled image: The blue regions represent the sea, the red and orange represent ships or boats and the yellow regions represent the docks.

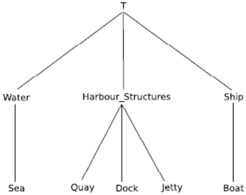

(c) Concept hierarchy T_C in the context of harbors.

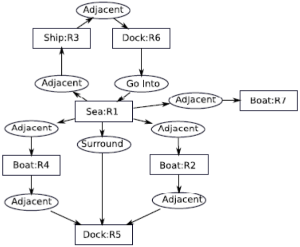

(d) Conceptual graph representing the spatial organization of some elements of Figure 5.8(b).

4. Mathematical morphology and deep learning

4.1 Combining Mathematical Morphology and Deep Learning

Morphological pre-processing

[Decencière et al., 2018]: Dealing with Topological Information within a Fully Convolutional Neural Network

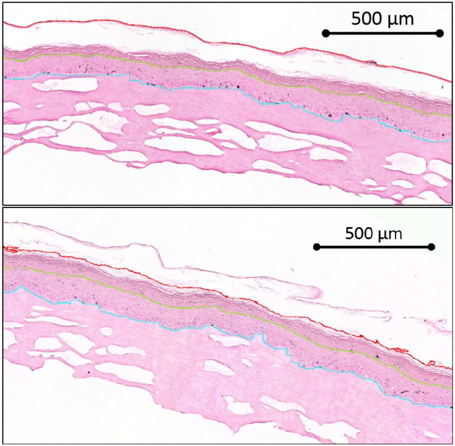

Morphological pre-processing

[Decencière et al., 2018]: Dealing with Topological Information within a Fully Convolutional Neural Network

A geodesical reconstruction adds non-local topological information.

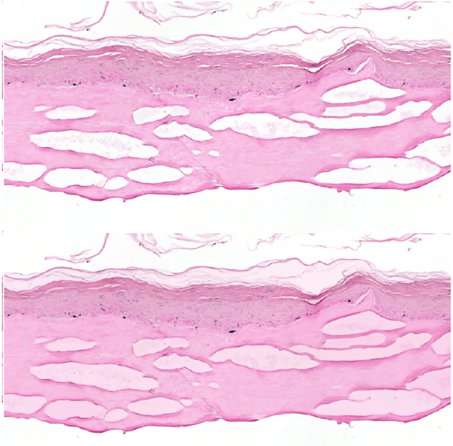

Morphological pre-processing

[Decencière et al., 2018]: Dealing with Topological Information within a Fully Convolutional Neural Network

A geodesical reconstruction adds non-local topological information.

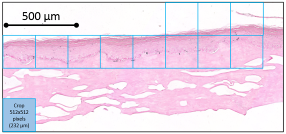

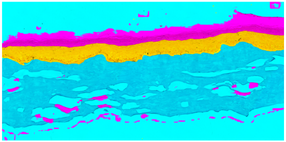
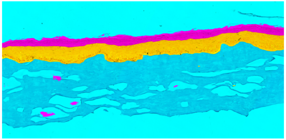

Left: input image ; **Middle:** Segmentation of a test image by a U-net trained on raw images (no pre-processing) ; **Right:** Segmentation of the same image by a U-net trained on pre-processed images where non-local topolgical information was included.

Morphological pre-processing

[Xu et al., 2018]: White Matter Hyperintensities Segmentation In a Few Seconds Using Fully Convolutional Network and Transfer Learning.

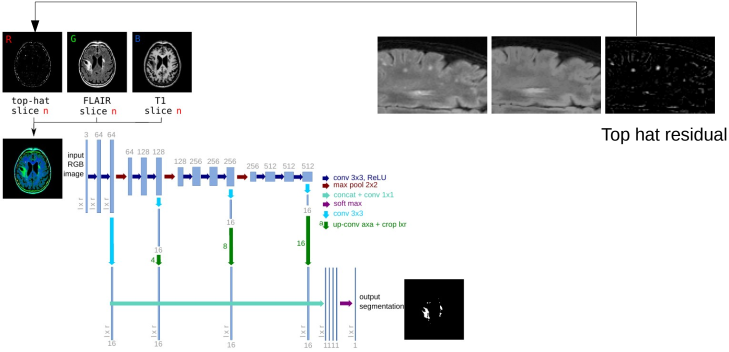

Fig. 2. Architecture of the proposed network. We fine tune it and combine linearly fine to coarse feature maps of the pre-trained VGG network [22]. Note that each color image (Input) is built from the slice n of the T1 and FLAIR sequences, and from a pre-processing result.

Morphological pre-processing

[Couteaux et al., 2019]: Automatic knee meniscus tear detection and orientation classification with Mask-RCNN

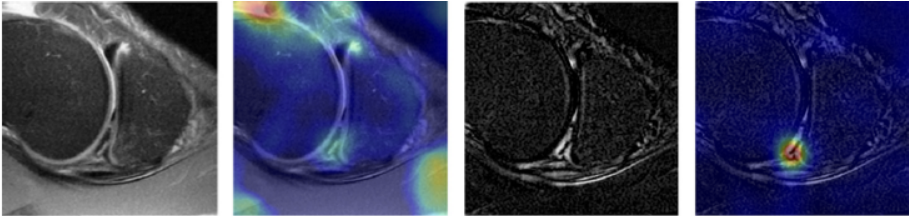

The input to the CNN is enhanced by a black top-hat, which improves explainability.

Morphological pseudo-labelling

Motivation: In many real life applications (industrial, bio-medical),

- a large amount of data is available
- but little is labelled (labelling is expensive)
- best performance are expected from supervised learning strategies (deep learning)

Can we train sophisticated models on cheap labelling and still get good performance?

"Cheap labelling": typically, by a non supervised algorithm (e.g. a morphological one).

Morphological pseudo-labelling

Example: Segmenting strands in high resolution X-ray computed tomography of 3D woven fabric

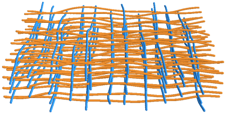

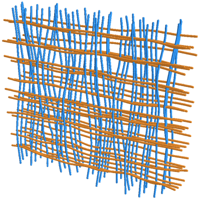

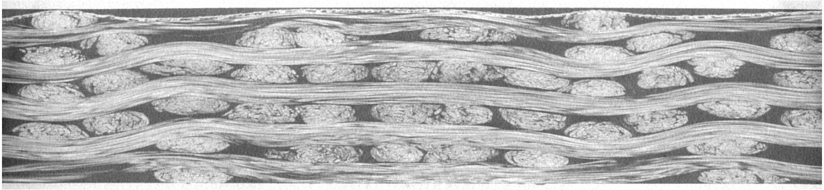

Morphological pseudo-labelling

Target segmentation

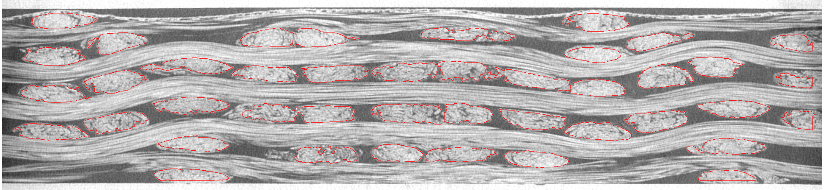

Labels available

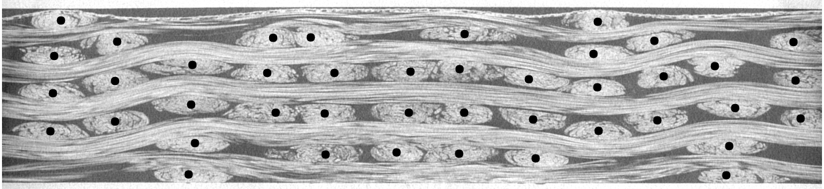

Morphological pseudo-labelling

A morphological pipeline to produce distance functions as pseudo-labels.

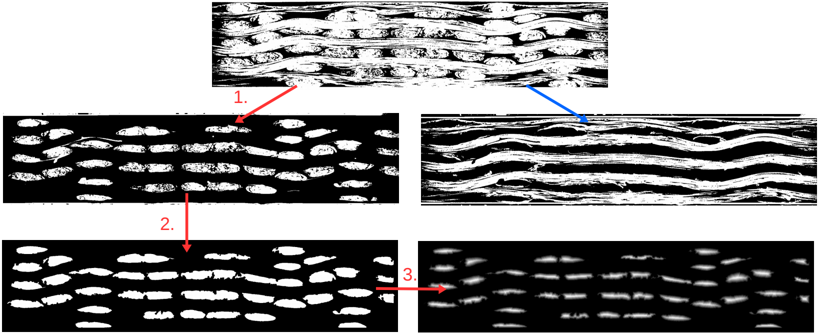

1. Adaptive anisotropic opening [Blusseau et al., 2018].
2. Classical morphological closings, fill holes.
3. Distance function, watershed transform and new distance function on each segment.

Morphological pseudo-labelling

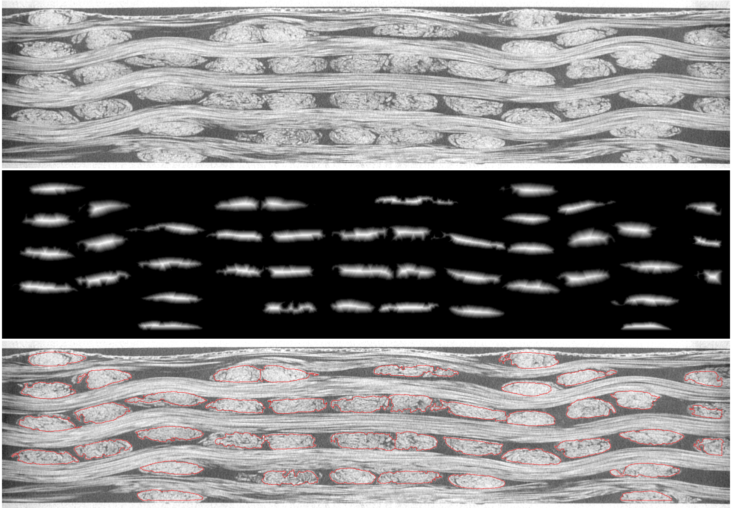

Top to bottom: Input, morphological processing used for pseudo-labelling, associated contours.

Morphological pseudo-labelling

A U-net is trained to compute pseudo distance functions on the morphological pseudo-labels.

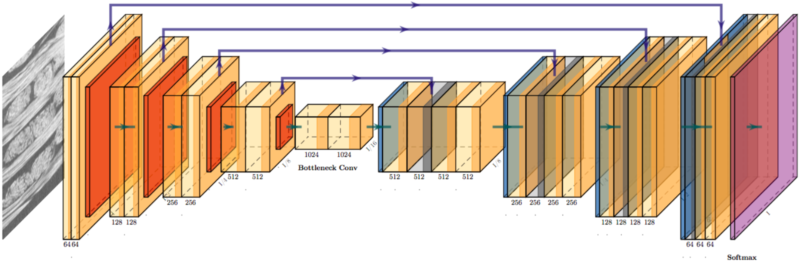

Morphological pseudo-labelling

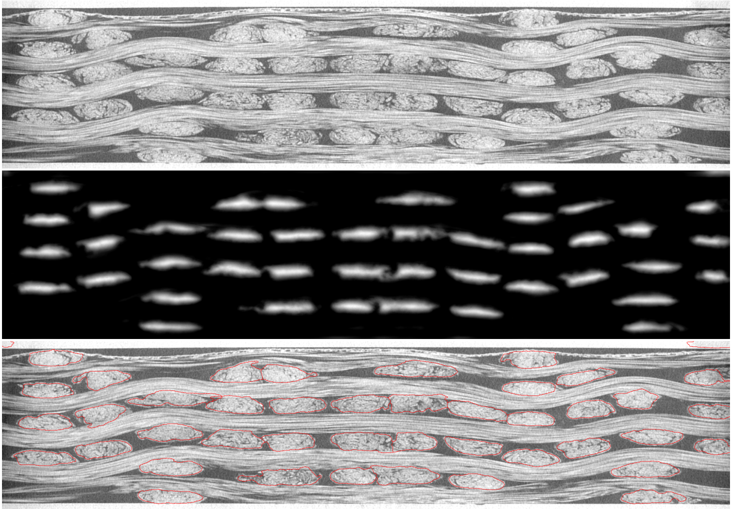

Top to bottom: Input, output of a U-net trained on the pseudo-labels, associated contours.

Morphological pseudo-labelling

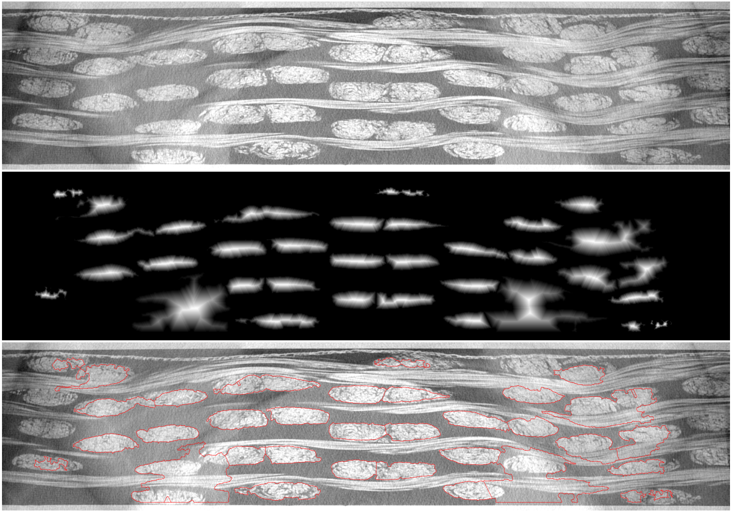

Top to bottom: Input, morphological processing used for pseudo-labelling, associated contours.

Morphological pseudo-labelling

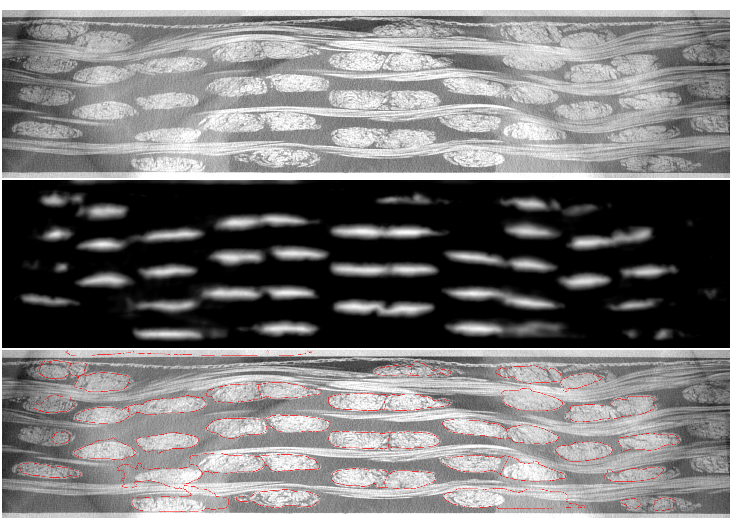

Top to bottom: Input, output of a U-net trained on the pseudo-labels, associated contours.

4.2 A short review on morphological neural networks

Probably the first paper on the topic

[Wilson, 1989]: Morphological networks

Weighted rank order filters

The weighted rank order filter will be defined informally as follows. The reference point of the structuring element is placed at an image pixel. That pixel value is changed by (a) adding the weights of the structuring elements to the corresponding pixels that the structuring element contacts, (b) ordering the resulting sums, and (c) choosing the Rth element in the ordered list as the output. The same notation as election will be used where the symbol Ξ implies a three dimensional structuring element.

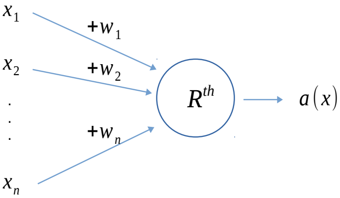

A neuron performs a weighted rank order filter:

$$a(\mathbf{x}) = ranked_R \{\mathbf{x}_i + \mathbf{w}_i,\ 1 \leq i \leq n\}$$

Probably the first paper on the topic

[Wilson, 1989]: Morphological networks

Figure 11.

Example of a rank trace in a multi-layer network.

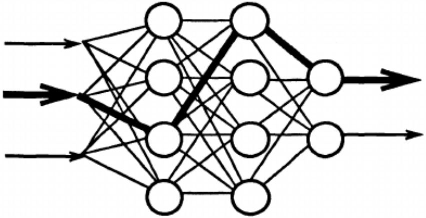

Neural networks without learning.

[Davidson and Ritter, 1990]: A theory of morphological neural networks

1. Introduction. The recent resurgence of interest in artificial neural networks has brought a deluge of publications to the field [4,9,15]. Applications of neural networks are appearing in a wider variety of fields each year. Recently, neural networks have been tied to a mathematical structure known as *image algebra* [14]. Image algebra was developed specifically for the concise expression and clear representation of image processing techniques and to provide a mathematical environment for image processing algorithm development, comparison, and optimization [5,12,13]. It has been shown that a subalgebra of the image algebra includes the mathematical formulations of currently popular neural network models [14], and image algebra expressions have been derived that represent some well-known algorithms designed for neural network computations. The neural network algorithms represented by these expressions look like their textbook formulations. These image algebra expressions are extremely simple and translucent, and the number of expressions representing each algorithm is very small. Furthermore, the image algebra has suggested a more general concept of neural computation than those that are currently used. In this paper we present a theory for a neural network that uses morphological operations. Several specific applications are given. In particular, we discuss networks that compute the morphological operations of opening and closing. We also give an example of a net that can perform the morphological operation of a sieve. A sieve is a morphological filter which filters out objects which are larger than a specified size [16].

We remark that an entirely different approach to a morphological network was presented in [17]. However, this particular model uses the usual operation of multiplication and summation at each node, a fundamental difference from the model presented here, which uses the operation of addition and maximum at each node.

17. S.S. Wilson, "Morphological Networks," in *Proc. of the 1989 SPIE Visual Comm. and Image Proc. IV*, Phila., PA (Nov., 1989).

Neural networks without learning.

[Davidson and Ritter, 1990]: A theory of morphological neural networks

$$\tau = \mathbf{a} \oplus \mathbf{t}$$

$$\mathbf{b} = f(\tau - \theta)$$

$$\mathbf{a} \oplus \mathbf{t} \equiv \{(\mathbf{y}, \mathbf{c}(\mathbf{y})) : \mathbf{c}(\mathbf{y}) = \sum_{\mathbf{x} \in \mathbf{X}} \mathbf{a}(\mathbf{x}) \cdot \mathbf{t}_{\mathbf{y}}(\mathbf{x}),\ \mathbf{y} \in \mathbf{Y}\}$$

$$\tau = \mathbf{a} \boxtimes \mathbf{t}$$

$$\mathbf{b} = f(\tau - \theta)$$

$$\mathbf{a} \boxtimes \mathbf{t} \equiv \{(\mathbf{y}, \mathbf{c}(\mathbf{y})) : \mathbf{c}(\mathbf{y}) = \bigvee_{\mathbf{x} \in \mathbf{X}} \mathbf{a}(\mathbf{x}) + \mathbf{t}_{\mathbf{y}}(\mathbf{x}),\ \mathbf{y} \in \mathbf{Y}\}$$

While in classical network models, the initial computation of τ (Equation II) is a linear process, the computation of τ in the model described by Equations VI and VIII is nonlinear. If the neural network model can be expressed using Equations VI and VII as the underlying equations of computation, we call it a *morphological neural network*. The remainder of this paper presents several specific morphological neural networks that can calculate openings, closings, and the boolean sieving filters as described by Serra [16].

Neural networks without learning.

[Davidson and Ritter, 1990]: A theory of morphological neural networks

A neuron performs a dilation:

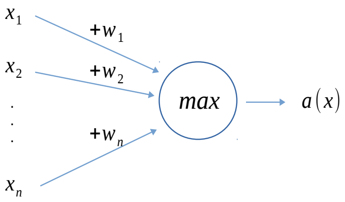

$$a(\mathbf{x}) = \max \{\mathbf{x}_i + \mathbf{w}_i,\ 1 \leq i \leq n\}$$

Learning dilations on images

[Davidson and Hummer, 1993]: Morphology neural networks: An introduction with applications.

Example 4. The Boolean Dilation Net with Learning.

The set of training data for this network consists of **P** pairs of images, $(\mathbf{a}^k, \mathbf{d}^k)$, $k = 0, \ldots, \mathbf{P} - 1$, where $\mathbf{a}^k$ represents the input image and $\mathbf{d}^k = \mathbf{a}^k \boxtimes \mathbf{t}$ is the input image dilated with an ideal (invariant) template **t**, which is the same for all images. In practical cases, the template **t** is assumed to be unknown.

Example 6. Grayscale Dilation with Learning for Variant Templates. This network is a generalization of nets in Examples 4 and 5, and is a more general form of the network in [5]. The additive maximum transform that this net attempts to learn can be any arbitrary grayscale one, including a variant transform. For a given set of P training data pairs, the learning rule needs about three passes through the data set to guarantee perfect recall of the P training images.

Learning dilations on images

[Davidson and Hummer, 1993]: Morphology neural networks: An introduction with applications.

Example 4. The Boolean Dilation Net with Learning.

case	a_i^k	d_j^k	c_j^k	new value for w_{ji} is
1	0	0	1	current value
2	0	1	0	current value
3	1 or 0	1	1	current value
4	1 or 0	0	0	current value
5	1	0	1	$-\infty$
6	1	1	0	0

Figure 5. Table of change-of-weight rules for boolean dilation network.

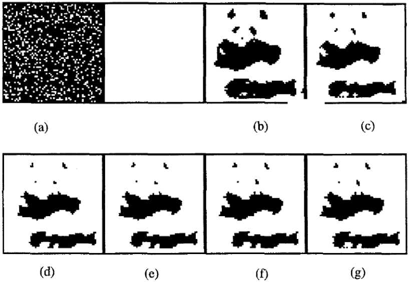

Figure 6. (a) Sample input training data; (b) sample natural scene (panda); (c) image in (b) dilated with von Neumann template; (d) output of net after X = 5 training images applied, for input of (b); (e) output of net after X = 10, for input of (b); (f) output of net after X = 15, for input of (b); (g) output of net after X = 20, for input of (b).

Learning dilations on images

[Davidson and Hummer, 1993]: Morphology neural networks: An introduction with applications.

Example 6. Grayscale Dilation with Learning for Variant Templates.

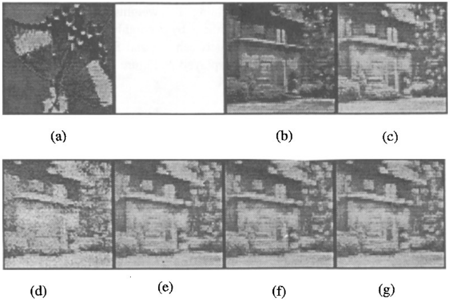

Figure 12. (a) One of the 13 training input images. (b) Test image. (c) Dilation of the test image by **t**. (d) Dilation of the test image by **w**(0). (e) Dilation of the test image by **w**(13). (f) Dilation of the test image by **w**(26). (g) Dilation of the test image by **w**(37) = **w**($3P-2$).

Learning *some* decision surfaces (two classes)

[Ritter and Sussner, 1996]: An introduction to morphological neural networks.

- Computing capabilities of Morphological Neural networks (can represent any boolean function)
- Morphological Associative Memories
- Single Layer Morphological Perceptron (SLMP): learning in finite steps but limited class of decision surfaces

$$\mathbf{p} = (p_1, p_2, \ldots, p_n) \in \mathbb{Z}^n \qquad W = \{w_1, w_2, \ldots, w_n\} \in \mathbb{Z}^n_{\pm\infty}$$

$$g(\mathbf{p}) = \bigvee_{i=1}^{n} [p_i + w_i]$$

$$f(x) = \begin{cases} 1 & if \ \ x > 0 \\ 0 & else \ . \end{cases}$$

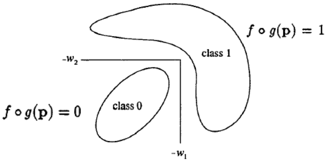

Fig. 3. Decision boundary for a single layer morphological perceptron.

Learning *any* decision surfaces (two classes)

[Sussner, 1998]: Morphological perceptron learning

- Generalized Single Layer Morphological Perceptron (SLMP)

$$f\left(\bigvee_{i=1}^{n} a_i\,(p_i + w_i)\right)$$

parameters $a_i \in \{1, -1\}$ are responsible for changing the signs of the sums $p_i + w_i$.

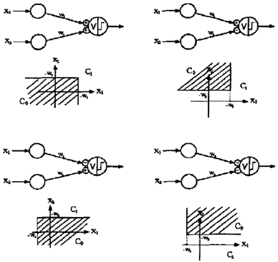

Figure 2:
Decision boundaries for different types of generalized single layer morphological perceptrons in the two-dimensional case.

Learning *any* decision surfaces (two classes)

[Sussner, 1998]: Morphological perceptron learning

- Multilayer Morphological perceptrons (MLMP): learning in finite steps and arbitrary decision surfaces (for 2 classes)

Finally, we present an algorithm for solving arbitrary instances of the 2-class problems by means of a two-layer morphological perceptron. Given a set of k training patterns in $\mathbb{R}^n$, this algorithm finds appropriate weights for a two-layer morphological perceptron such that each of the training patterns is correctly classified by the two-layer morphological perceptron. This algorithm also determines how many nodes in the hidden layer are necessary in order to solve the given problem.

Learning in conventional multilayer perceptrons can be achieved by minimizing a certain error function which depends on the weights. Finding the global minimum of this error function is a very difficult task, and is not always possible. Weight training in multilayer morphological perceptrons does not encounter such limitations.

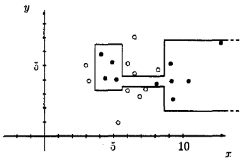

Figure 6:
Decision surface found by learning algorithm.

Improving the learning of hyperboxes with SGD

[Zamora and Sossa, 2017]: Dendrite morphological neurons trained by stochastic gradient descent.

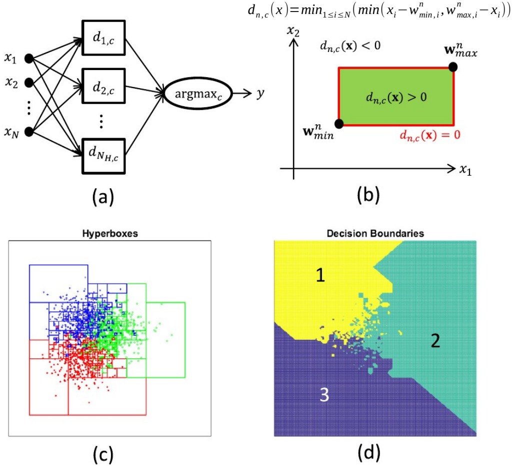

[Zamora and Sosa, 2017]: Dendrite morphological neurons trained by stochastic gradient descent.

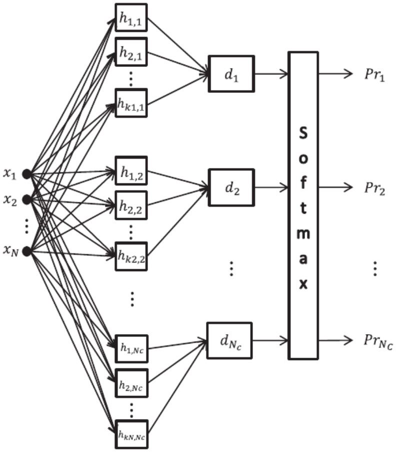

Fig. 3. Neural architecture for a DMN with a softmax layer. Each class corresponds to one dendrite cluster d_c.

$$h_{k,c}(\mathbf{x}) = \min\left(\min\left(\mathbf{x} - \mathbf{w}_{k,c}, \mathbf{w}_{k,c} + \mathbf{b}_{k,c} - \mathbf{x}\right)\right)$$

$$d_c(\mathbf{x}) = \max_k \left(h_{k,c}(\mathbf{x})\right)$$

$$Pr_c(\mathbf{x}) = \frac{\exp\left(d_c(\mathbf{x})\right)}{\sum_{k=1}^{N_C} \exp\left(d_k(\mathbf{x})\right)}$$

$$y = \arg\max_c (Pr_c(\mathbf{x}))$$

Between linear and morphological networks.

[Pessoa and Maragos, 2000]: Neural networks with hybrid morphological/rank/linear nodes: a unifying framework with applications to handwritten character recognition.

$$z_n^{(l)} \equiv \lambda_n^{(l)}\alpha_n^{(l)} + (1-\lambda_n^{(l)})\beta_n^{(l)},$$

$$\alpha_n^{(l)} = \mathscr{R}_{r_n^{(l)}}(\mathbf{y}^{(l-1)} + \mathbf{a}_n^{(l)}),$$

$$\beta_n^{(l)} = \mathbf{y}^{(l-1)} \cdot (\mathbf{b}_n^{(l)})' + \tau_n^{(l)},$$

where $\lambda_n^{(l)}, \tau_n^{(l)} \in \mathbb{R}$; $\mathbf{a}_n^{(l)}, \mathbf{b}_n^{(l)} \in \mathbb{R}^{N_{l-1}}$.

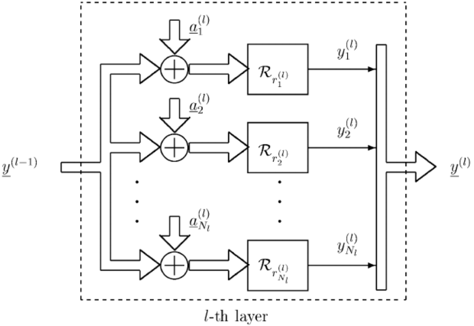

Fig. 2. Structure of the lth layer in an MRNN.

[Pessoa and Maragos, 2000]: Neural networks with hybrid morphological/rank/linear nodes: a unifying framework with applications to handwritten character recognition.

An example in two dimensions:

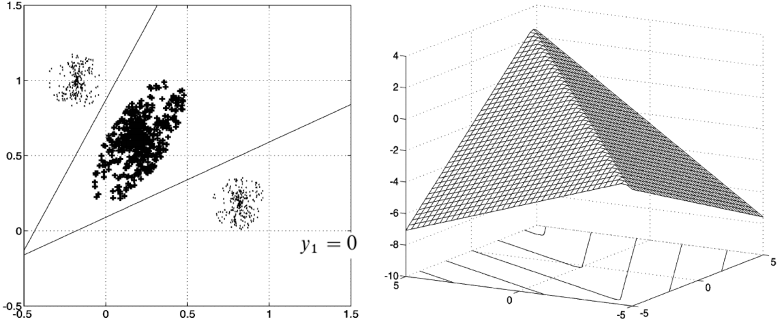

(a) (b)

$$y_1 = \lambda \min\{x_1 + a_1, x_2 + a_2\}$$
$$+ (1 - \lambda)(x_1 b_1 + x_2 b_2 + \tau_1).$$

[Pessoa and Maragos, 2000]: Neural networks with hybrid morphological/rank/linear nodes: a unifying framework with applications to handwritten character recognition.

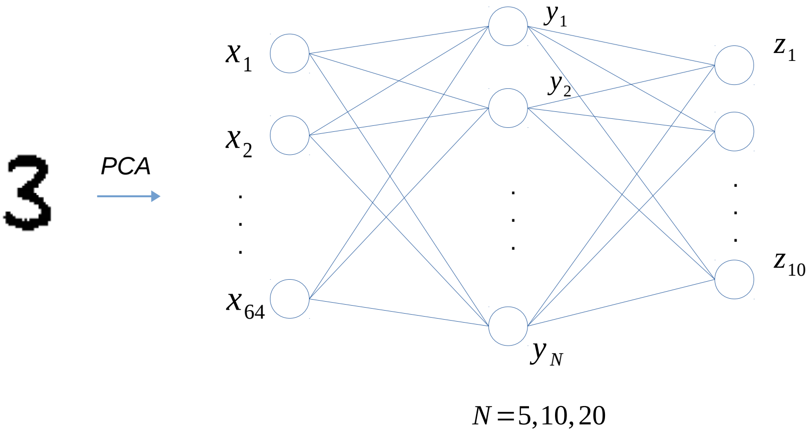

MLP and MRL nets compared: similar performance with faster convergence for MRLs.

Dense max-plus layers to prune networks

Seminal experiment by [Charisopoulos and Maragos, 2017].

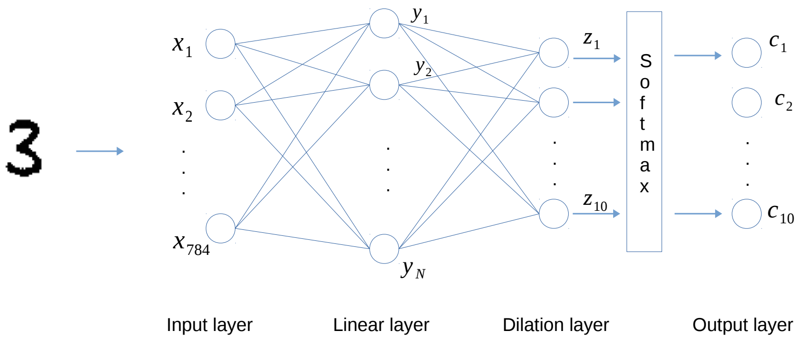

$y_i = \sum_{j=1}^{784} w_{ij} x_j$ $\quad z_k = max_{1 \le i \le N} \{\alpha_{ik} + y_i\}$

Classification of the MNIST dataset.

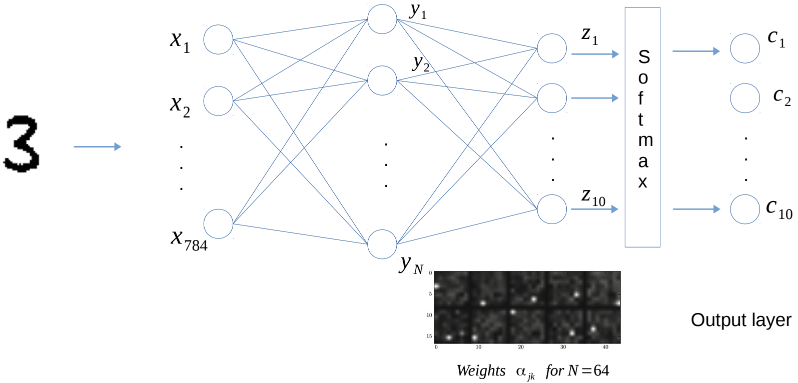
x_1
x_2
x_{784}
y_1
y_2
y_N
z_1
z_{10}
Softmax
c_1
c_2
c_{10}
Output layer
Weights α_{jk} for $N=64$

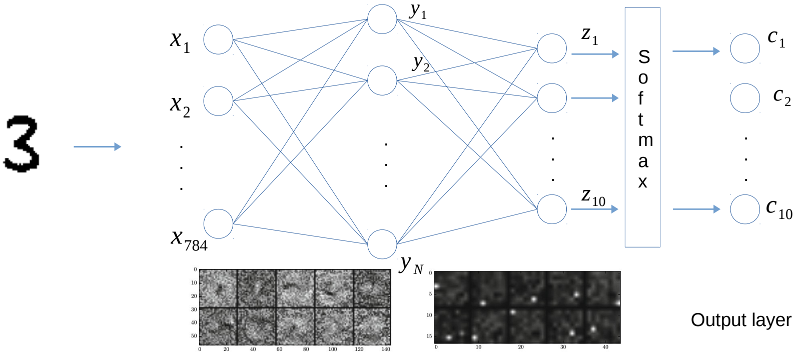

Weights w_{ij} *for the* 10 *active filters* *Weights* α_{jk} *for* $N = 64$

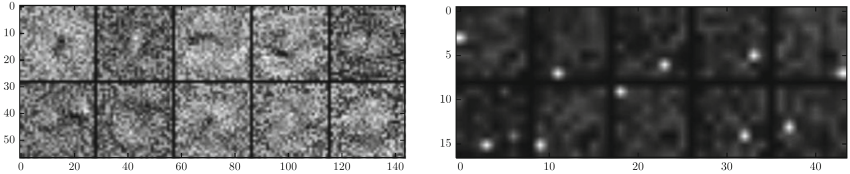

Weights of the two layers in the previous architecture [Charisopoulos and Maragos, 2017], after training on the MNIST dataset.

Left: weights w_{ij} of the 10 *active* linear filters. **Right:** weights α_{jk} of the max-plus layer for $N = 64$ units in the previous layer.

Extended study by [Zhang et al., 2019].

- Adding dropout:

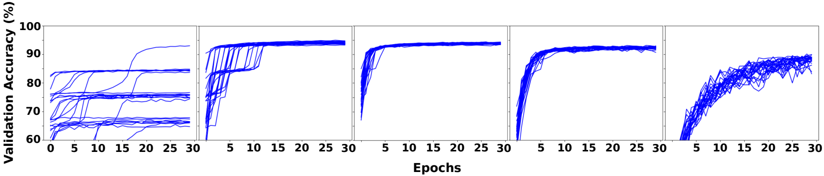

(a) Dropout : 0% (b) 25% (c) 50% (d) 75% (e) 90%

Classification accuracy per epochs for 25 runs with different random initializations and dropout ratios on MNIST validation set.

Extended study by [Zhang et al., 2019].

- Interpretation of max-plus blocks as “dynamic” Maxout units [Goodfellow et al., 2013]:

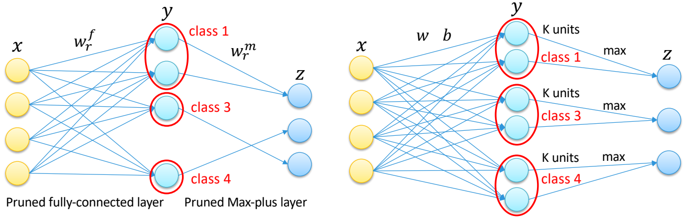

Illustration of the comparison between the pruned Max-plus model (left) and Maxout model (right).

Extended study by [Zhang et al., 2019].

- Pruning deeper CNNs for more complex data:

CNN	Max-plus	Pruned Max-plus
conv(5*5)	conv(5*5)	conv(5*5)
maxpool(2*2)	maxpool(2*2)	maxpool(2*2)
conv(5*5)	conv(5*5)	conv(5*5)
maxpool(2*2)	maxpool(2*2)	maxpool(2*2)
fc(384)	fc(384)	fc(384)
fc(192)	fc(192)	fc(10)
fc(10)	maxplus(10)	maxplus(10)
83.5%	83.9%	83.9%

The architecture of the CNN model, unpruned and pruned Max-plus model, along with their performance on the test set of CIFAR-10 dataset.

Convolutional-like morphological networks

[Franchi et al., 2020]: Deep morphological networks.

- Morphological layers instead of convolutional layers (shared weights)
- Learned structuring elements (morphological counterpart of the kernel filters)
- Gradient based optimization using modern tools (Tensorflow)
- Adaptive pooling, classification, denoising, edge detection

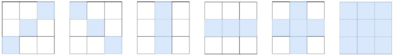

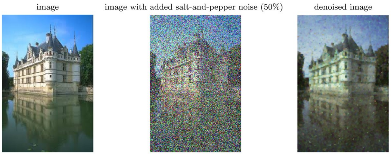

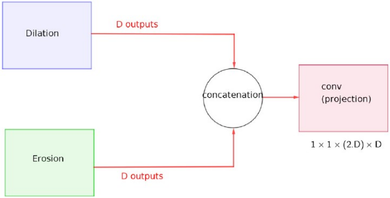

Fig. 3. The morphological pooling operator. The erosion and dilation share the same structuring element and are applied in parallel to the input data. The results of these morphological operators are concatenated and projected back to the original size with a 1 × 1 convolution.

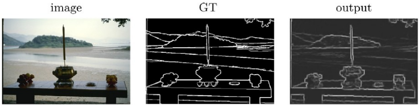

4.3 Deep morphological networks in practice

Code tutorial 1: pruning a network with a max-plus dense layer

Architecture: "max-plus block" [Zhang et al., 2019]

$\mathbf{x} \in \mathbb{R}^I, \ \mathbf{y} \in \mathbb{R}^J, \ \mathbf{z} \in \mathbb{R}^K, \ \mathbf{w}^f \in \mathbb{R}^{I \times J}, \ \mathbf{w}^m \in \mathbb{R}_{max}^{J \times K},$

$$\begin{aligned} \mathbf{y}_j &= \sum_{i=1}^{I} \mathbf{x}_i \cdot \mathbf{w}^f_{ij} \\ \mathbf{z}_k &= \max_{1 \leq j \leq J} \left\{ \mathbf{y}_j + \mathbf{w}^m_{jk} \right\}. \end{aligned}$$

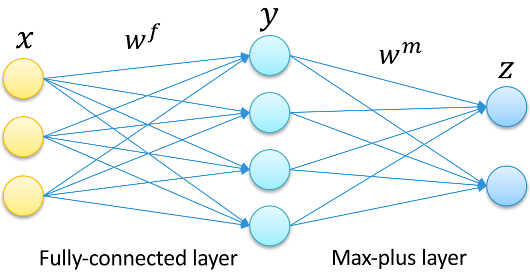

Code tutorial 1: pruning a network with a max-plus dense layer

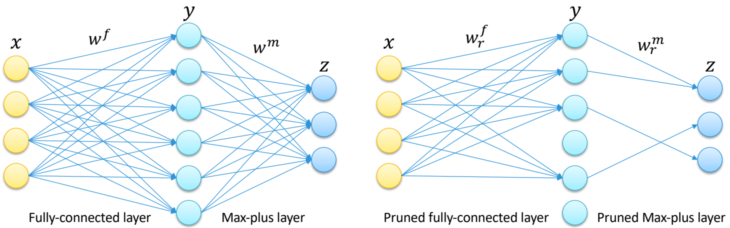

Illustration of the comparison between the original Max-plus block (left) and the pruned Max-plus block (right).

- Tutorial based on code available at `https://github.com/samyblusseau/maxplusblock`.
- The notebook running on Google Colaboratory is at `https://cloud.mines-paristech.fr/index.php/s/BEZIx6s7uZWqXxW`

Code tutorial 2: training a morphological network like a CNN

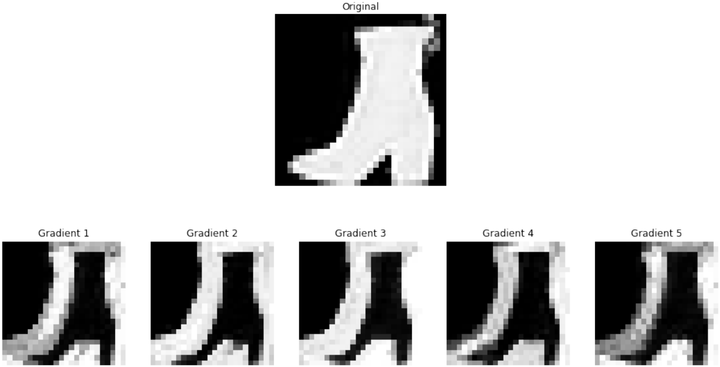

- Tutorial based on code bdeveloped y Santiago Velasco-Forero, available at `http://www.cmm.mines-paristech.fr/~velasco/morpholayers/intro.html`.
- The notebook running on Google Colaboratory is at `https://cloud.mines-paristech.fr/index.php/s/BEZIx6s7uZWqXxW`

Conclusion

- Algebraic framework of mathematical morphology.
- Strong properties.
- Natural links with logics.
- Applies in different frameworks (many types of logics, fuzzy sets, bipolarity, graphs and hypergraphs, formal concept analysis...).
- Knowledge representation.
- Reasoning (on preferences, on beliefs, on spatial information...).
- Both symbolic and numerical.
- Combination with machine learning and deep learning.

References I

Aiguier, M., Atif, J., Bloch, I., and Hudelot, C. (2018a).
Belief revision, minimal change and relaxation: A general framework based on satisfaction systems, and applications to description logics.
Artificial Intelligence, 256:160–180.

Aiguier, M., Atif, J., Bloch, I., and Pérez, R. P. (2018b).
Explanatory relations in arbitrary logics based on satisfaction systems, cutting and retraction.
International Journal of Approximate Reasoning, 102:1–20.

Aiguier, M. and Bloch, I. (2019).
Logical dual concepts based on mathematical morphology in stratified institutions: applications to spatial reasoning.
Journal of Applied Non-Classical Logics, 29(4):392–429.

Alchourron, C., Gardenfors, P., and Makinson, D. (1985).
On the logic of theory change.
Journal of Symbolic Logic, 50(2):510–530.

References II

Atif, J., Hudelot, C., and Bloch, I. (2014).
Explanatory reasoning for image understanding using formal concept analysis and description logics.
IEEE Transactions on Systems, Man, and Cybernetics: Systems, 44(5):552–570.

Bloch, I. (2002).
Modal logics based on mathematical morphology for qualitative spatial reasoning.
Journal of Applied Non-Classical Logics, 12(3-4):399–423.

Bloch, I. (2005).
Fuzzy Spatial Relationships for Image Processing and Interpretation: A Review.
Image and Vision Computing, 23(2):89–110.

Bloch, I. (2017).
Topological relations between bipolar fuzzy sets based on mathematical morphology.
In *International Symposium on Mathematical Morphology (ISMM 2017)*, volume LNCS 10225, pages 40–51, Fontainebleau, France.

Bloch, I., Heijmans, H., and Ronse, C. (2007).
Mathematical Morphology.
In Aiello, M., Pratt-Hartman, I., and van Benthem, J., editors, *Handbook of Spatial Logics*, chapter 13, pages 857–947. Springer.

References III

Bloch, I. and Lang, J. (2000).
Towards Mathematical Morpho-Logics.
In *8th International Conference on Information Processing and Management of Uncertainty in Knowledge based Systems IPMU 2000*, volume III, pages 1405–1412, Madrid, Spain.

Bloch, I. and Lang, J. (2002).
Towards Mathematical Morpho-Logics, pages 367–380.
Physica-Verlag HD, Heidelberg.

Bloch, I., Lang, J., Pino Pérez, R., and Uzcátegui, C. (2018).
Morphologic for knowledge dynamics: revision, fusion, abduction.
Technical Report arXiv:1802.05142, arXiv cs.AI.

Bloch, I., Pérez, R. P., and Uzcátegui, C. (2004).
A unified treatment for knowledge dynamics.
In *KR*, pages 329–337.

Bloch, I., Pérez, R. P., and Uzcategui, C. (2006).
Mediation in the Framework of Morphologic.
In *European Conference on Artificial Intelligence ECAI 2006*, pages 190–194, Riva del Garda, Italy.

References IV

Bloch, I., Pino-Pérez, R., and Uzcátegui, C. (2001).
Explanatory relations based on mathematical morphology.
In *European Conference on Symbolic and Quantitative Approaches to Reasoning and Uncertainty*, pages 736–747. Springer.

Blusseau, S., Velasco-Forero, S., Angulo, J., and Bloch, I. (2018).
Tropical and morphological operators for signal processing on graphs.
In *25th IEEE International Conference on Image Processing (ICIP)*, pages 1198–1202.

Charisopoulos, V. and Maragos, P. (2017).
Morphological perceptrons: geometry and training algorithms.
In *International Symposium on Mathematical Morphology and Its Applications to Signal and Image Processing*, pages 3–15.

Couteaux, V., Si-Mohamed, S., Nempont, O., Lefevre, T., Popoff, A., Pizaine, G., Villain, N., Bloch, I., Cotten, A., and Boussel, L. (2019).
Automatic knee meniscus tear detection and orientation classification with mask-rcnn.
Diagnostic and Interventional Imaging, 100(4):235 – 242.

Davidson, J. L. and Hummer, F. (1993).
Morphology neural networks: An introduction with applications.
Circuits, Systems and Signal Processing, 12(2):177–210.

References V

Davidson, J. L. and Ritter, G. X. (1990).
Theory of morphological neural networks.
In *Digital Optical Computing II*, volume 1215, pages 378–389.

Decencière, E., Velasco-Forero, S., Min, F., Chen, J., Burdin, H., Gauthier, G., Laÿ, B., Bornschloegl, T., and Baldeweck, T. (2018).
Dealing with topological information within a fully convolutional neural network.
In Blanc-Talon, J., Helbert, D., Philips, W., Popescu, D., and Scheunders, P., editors, *Advanced Concepts for Intelligent Vision Systems*, pages 462–471, Cham. Springer International Publishing.

Delmonte, A., Bloch, I., Hasboun, D., Mercier, C., Pallud, J., and Gori, P. (2018).
Segmentation of white matter tractograms using fuzzy spatial relations.
In *Human Brain Mapping (OHBM)*, Singapore.

Fouquier, G., Atif, J., and Bloch, I. (2012).
Sequential model-based segmentation and recognition of image structures driven by visual features and spatial relations.
Computer Vision and Image Understanding, 116(1):146–165.

References VI

Franchi, G., Fehri, A., and Yao, A. (2020).
Deep morphological networks.
Pattern Recognition, 102:107246.

Goodfellow, I. J., Warde-Farley, D., Mirza, M., Courville, A., and Bengio, Y. (2013).
Maxout networks.
arXiv preprint arXiv:1302.4389.

Gorogiannis, N. and Hunter, A. (2008a).
Implementing semantic merging operators using binary decision diagrams.
International Journal of Approximate Reasoning, 49(1):234–251.

Gorogiannis, N. and Hunter, A. (2008b).
Merging First-Order Knowledge using Dilation Operators.
In *Fifth International Symposium on Foundations of Information and Knowledge Systems, FoIKS'08*, volume LNCS 4932, pages 132–150.

Heijmans, H. and Ronse, C. (1990).
The algebraic basis of mathematical morphology i. dilations and erosions.
Computer Vision, Graphics, and Image Processing, 50(3):245 – 295.

References VII

Hudelot, C., Atif, J., and Bloch, I. (2008).
Fuzzy spatial relation ontology for image interpretation.
Fuzzy Sets and Systems, 159(15):1929–1951.

Katsuno, H. and Mendelzon, A.-O. (1991).
Propositional knowledge base revision and minimal change.
Artificial Intelligence, 52:263–294.

Konieczny, S. and Pino Pérez, R. (2011).
Logic based merging.
Journal of Philosophical Logic, 40(2):239–270.

Landini, G., Galton, A., Randell, D., and Fouad, S. (2019).
Novel applications of discrete mereotopology to mathematical morphology.
Signal Processing: Image Communication, 76:109 – 117.

Matheron, G. (1967).
Eléments pour une théorie des milieux poreux.
Masson, Paris.

Matheron, G. (1975).
Random Sets and Integral Geometry.
Wiley, New-York.

References VIII

Muller, C., Delmonte, A., Meignan, P., Peyrot, Q., Virzi, A., Berteloot, L., Grevent, D., Blanc, T., Gori, P., Boddaert, N., Bloch, I., and Sarnacki, S. (2019).
Nervous system exploration using tractography to enhance pelvic surgery.
In *Surgetica*, pages 90–92, Rennes, France.

Nempont, O., Atif, J., and Bloch, I. (2013).
A constraint propagation approach to structural model based image segmentation and recognition.
Information Sciences, 246:1–27.

Pessoa, L. F. and Maragos, P. (2000).
Neural networks with hybrid morphological/rank/linear nodes: a unifying framework with applications to handwritten character recognition.
Pattern Recognition, 33(6):945–960.

Pino Pérez, R. and Uzcátegui, C. (2003).
Preferences and explanations.
Artificial Intelligence, 149(1):1–30.

Ritter, G. X. and Sussner, P. (1996).
An introduction to morphological neural networks.
In *13th International Conference on Pattern Recognition*, volume 4, pages 709–717.

References IX

Serra, J. (1982).
Image Analysis and Mathematical Morphology.
Academic Press, London.

Serra, J. (1988).
Image Analysis and Mathematical Morphology, Part II: Theoretical Advances.
Academic Press (J. Serra Ed.), London.

Sussner, P. (1998).
Morphological perceptron learning.
In *Proceedings of the 1998 IEEE International Symposium on Intelligent Control (ISIC) held jointly with IEEE International Symposium on Computational Intelligence in Robotics and Automation (CIRA) Intell*, pages 477–482. IEEE.

Vanegas, M.-C., Bloch, I., and Inglada, J. (2016).
Fuzzy constraint satisfaction problem for model-based image interpretation.
Fuzzy Sets and Systems, 286:1–29.

Wilson, S. S. (1989).
Morphological networks.
In *Visual Communications and Image Processing IV*, volume 1199, pages 483–496.

References X

Xu, Y., Géraud, T., Puybareau, É., Bloch, I., and Chazalon, J. (2018).
White matter hyperintensities segmentation in a few seconds using fully convolutional network and transfer learning.
In Crimi, A., Bakas, S., Kuijf, H., Menze, B., and Reyes, M., editors, *Brainlesion: Glioma, Multiple Sclerosis, Stroke and Traumatic Brain Injuries*, pages 501–514, Cham. Springer International Publishing.

Zamora, E. and Sossa, H. (2017).
Dendrite morphological neurons trained by stochastic gradient descent.
Neurocomputing, 260:420–431.

Zhang, Y., Blusseau, S., Velasco-Forero, S., Bloch, I., and Angulo, J. (2019).
Max-plus operators applied to filter selection and model pruning in neural networks.
In *International Symposium on Mathematical Morphology and Its Applications to Signal and Image Processing*, pages 310–322. Springer.